Original Article

Calcification circumference, area, and location are associated with carotid stent expansion rate: high-resolution magnetic resonance vessel wall imaging study

Yumeng Sun[1]^, Haiyang Xu[1], Lei Kou[2], Shuo Wang[2], Zhenjia Wang[3], Wei Yu[1]

[1]Department of Radiology, Beijing Anzhen Hospital, Beijing, China; [2]Department of Vascular Surgery, Beijing Anzhen Hospital, Beijing, China; [3]Department of Radiology, Beijing Hospital of Traditional Chinese Medicine, Beijing, China

Contributions: (I) Conception and design: Y Sun, W Yu; (II) Administrative support: W Yu; (III) Provision of study materials or patients: S Wang, L Kou; (IV) Collection and assembly of data: Y Sun, H Xu, Z Wang; (V) Data analysis and interpretation: Y Sun, W Yu; (VI) Manuscript writing: All authors; (VII) Final approval of manuscript: All authors.

Correspondence to: Wei Yu, MD. Department of Radiology, Beijing Anzhen Hospital, No. 2, Anzhen Road, Chaoyang District, Beijing 100029, China. Email: nxyw1969@163.com.

Background: The plaque imaging findings associated with the stent expansion rate (SER) of the carotid artery are not well known. The purpose of this study was to investigate the imaging findings associated with SER.

Methods: It was a retrospective investigation. Based on the kind of carotid stents used, retrospective data from 89 patients who had carotid artery stenting (CAS) for atherosclerotic carotid stenosis were gathered and divided into two groups: open-cell stents and closed-cell stents. Patients underwent preoperative carotid high-resolution magnetic resonance vessel wall imaging (HR-VWI). Use HR-VWI to quantitatively evaluate carotid wall thickness and plaque components. Calculate SER using digital subtraction angiography (DSA). All patients' baseline and HR-VWI imaging features were retrospectively analyzed. Simple and multivariable linear regression analysis was used to determine the imaging findings associated with SER of open-cell and closed-cell stents.

Results: A total of 89 patients (mean age, 70±8 years; 69 men) were included in the final analysis. Among 89 patients, 35 patients were treated with open-cell stents. Fifty-four patients were treated with closed-cell stents. In the open-cell stents group, the Maximum single-slice calcification circumference score, maximum wall thickness (WT_{max}), and total calcification location score with P<0.10 in the simple linear regression analysis were included in the multivariable linear regression analysis. The results of the multivariable linear regression revealed that only the Maximum single-slice calcification circumference score (β=–9.35; 95% CI: –18.15 to –0.56; P=0.03) was associated with SER of open-cell stents. In the closed-cell stents group, the Maximum single-slice calcification circumference score, WT_{max}, maximum area percentage of calcification, calcification volume, and total calcification location score with P<0.10 in the simple linear regression analysis were included in the multivariable linear regression analysis. The results of the multivariable linear regression revealed that the Maximum area percentage of calcification (β=–0.67; 95% CI: –1.29 to –0.05; P=0.03), Maximum single-slice calcification circumference score (β=–8.43; 95% CI: –13.36 to –3.49; P=0.001) and total calcification location score (β=–0.37; 95% CI: –1.08 to 0.09; P=0.02) were associated with SER of closed-cell stents.

Conclusions: Calcified plaques are associated with SER of the carotid artery. Calcification circumference correlates with SER of open-cell stents. Calcification circumference, calcification area, and calcification

^ ORCID: 0000-0002-6005-5412.

location are related to SER of closed-cell stents, which may provide a new consideration for clinicians when choosing carotid artery stents.

Keywords: Carotid artery stenting (CAS); stent expansion rate; high-resolution magnetic resonance vessel wall imaging; calcification

Submitted Nov 03, 2022. Accepted for publication Apr 20, 2023. Published online May 08, 2023.
doi: 10.21037/qims-22-1215
View this article at: https://dx.doi.org/10.21037/qims-22-1215

Introduction

Carotid stenosis or occlusion is one of the main causes of ischemic stroke (1). The previous randomized controlled trial has shown that there was no discernible difference between the carotid endarterectomy (CEA) group and the carotid artery stenting (CAS) group in the estimated 4-year rates of the primary endpoint (stroke, myocardial infarction, or death) [7.2% and 6.8%, respectively; hazard ratio with stenting, 1.11; 95% confidence interval (CI): 0.81–1.51; P=0.51], which reveals CAS as a potential alternative to CEA (2). Stroke and myocardial infarction are one of the major perioperative complications of CEA and CAS. However, the incidence of major complications in the perioperative period was different between CEA and CAS. There was a greater risk of stroke with CAS (CAS *vs.* CEA: 4.1% *vs.* 3.3%, P=0.01) and a higher risk of myocardial infarction with CEA (CAS *vs.* CEA: 1.1% *vs.* 2.3%, P=0.03) during the periprocedural period (2).

Residual stenosis is an independent risk factor for restenosis and can affect the long-term outcome after stenting (3-5). A recent study showed that the overall incidence of residual stenosis was 22.8% (130/570 stents) and restenosis occurs in 13% of patients with residual stenosis during follow-up (6). The study also noted that plaque morphology, calcified plaque, and stent type are risk factors for residual stenosis. On the contrary, a high stent expansion rate was a protective factor for residual stenosis (6). The stent expansion rate (SER) is defined as the difference between the preoperative stenosis rate of the carotid artery and the residual stenosis rate post-stenting, reflecting the expansion ability of the stent (6). Previous studies found that open- and closed-cell stents have different mechanical properties due to differences in design and materials (7-9). The radial force of closed-cell stents was significantly lower than that of open-cell stents (7,8). However, the plaque imaging findings associated with SER of open-cell and closed-cell stents are unknown, and the clinical significance of the SER is also unclear.

To assess the carotid plaque, high-resolution magnetic resonance vessel wall imaging (HR-VWI) has already been used extensively, as it enables the visualization of plaque composition *in vivo* and provides important insight into plaque vulnerability rather than the degree of stenosis alone (10-12). It is also an excellent method for assessing calcification with an accuracy of 98% and a specificity of 99% (13). The purpose of this study was to quantitatively evaluate carotid plaque by HR-VWI and to investigate the imaging findings related to SER of open-cell and closed-cell stents.

Methods

Study patients

This was a retrospective study. The study was conducted in accordance with the Declaration of Helsinki (as revised in 2013). The study was approved by the ethics board of Beijing Anzhen Hospital, Beijing, China (No. 2022135X), and individual consent for this retrospective analysis was waived. Patients who underwent HR-VWI in our hospital between January 2018 and April 2021 and met the following inclusion criteria were enrolled retrospectively: (I) patients had symptomatic carotid stenosis of ≥50% or asymptomatic carotid artery stenosis of ≥70% according to the North American Symptomatic Carotid Endarterectomy Trial (NASCET) criteria (14); (II) patients had their first CAS treatment; (III) patients underwent HR-VWI within 1 week before CAS; (IV) patients had complete clinical data and satisfactory HR-VWI imaging quality. Clinical data include age, sex, hypertension, hyperlipidemia, diabetes, coronary artery disease, history of stroke, smoking, stent type, pre-dilatation balloon frequency, post-dilatation balloon, and preoperative stenosis rate of the carotid artery. According to the clarity and contrast between the vascular wall and the surrounding cerebrospinal fluid (CSF) or blood by

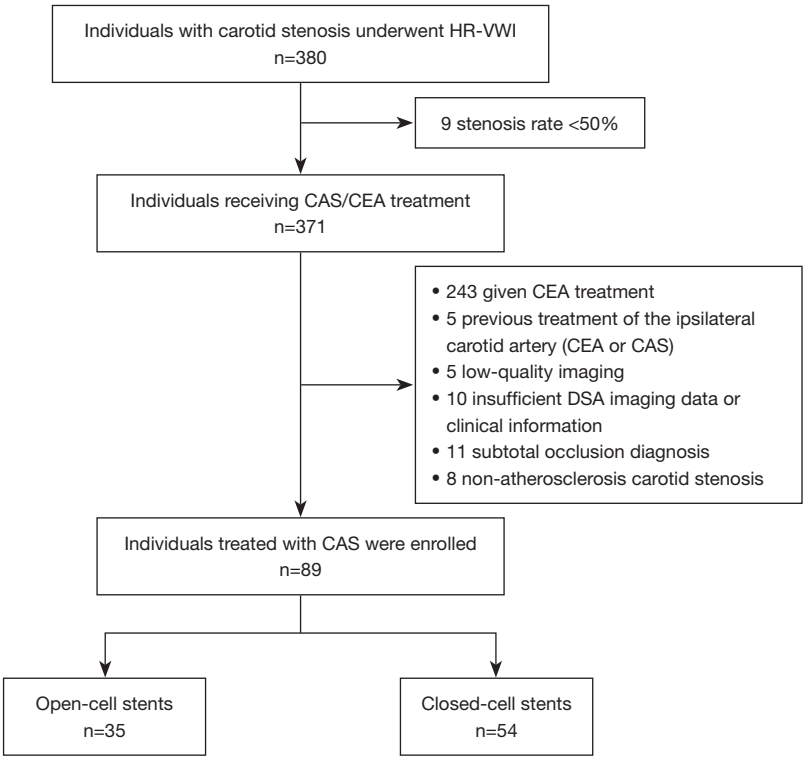

Figure 1 The flow chart of the study. HR-VWI, high-resolution magnetic resonance vessel wall imaging; CAS, carotid artery stenting; CEA, carotid endarterectomy; DSA, digital subtraction angiography.

eyeballing, the HR-VWI image quality was graded using a 4-point scale as follows: 1, poor; 2, marginal; 3, good; and 4, excellent. For subsequent analysis, only the HR-VWI images with IQ ≥2 were used (15). The exclusion criteria included the following: (I) patients were treated with CEA; (II) prior carotid artery procedures (CEA or CAS); (III) carotid occlusion; (IV) nonatherosclerotic carotid stenosis; (V) incomplete clinical data/insufficient HR-VWI image quality. Patients were divided into open-cell stents and closed-cell stents groups based on the type of carotid stents (*Figure 1*). A retrospective analysis was done on the clinical and HR-VWI imaging data of the patients enrolled.

HR-VWI imaging and analysis

Carotid HR-VWI was performed on a 3.0T MR scanner (Ingenia CX, R541 software version, Philips Healthcare, Best, Netherlands) with a combination of a 32-channel head coil (Philips Healthcare) and an 8-channel neck coil (TSImaging Healthcare, Beijing, China). The imaging protocol included two-dimensional T1-weighted imaging (2D T1WI) (turbo spin echo; repetition time/echo time =800/10 ms; flip angle =90°; field of view =16×16 cm^2; resolution =0.6×0.6 mm^2; slice thickness =2 mm; number of slices =20), two-dimensional T2-weighted imaging (2D T2WI) (turbo spin echo; repetition time/echo time =4,800/50 ms; flip angle =90°; field of view =16×16 cm^2; resolution =0.6×0.6 mm^2; slice thickness =2 mm; number of slices =20), three-dimensional time of flight-magnetic resonance angiography (3D TOF-MRA) (fast-field echo; repetition time/echo time =20/4 ms; flip angle =20°; field of view =16×16 cm^2; resolution =0.6×0.6 mm^2; slice thickness =2 mm; number of slices =40), and 3D simultaneous non-contrast angiography and intraplaque hemorrhage (SNAP) sequences (turbo field echo; repetition time/echo time =12/6.8 ms; flip angle =5°; field of view =16×16 cm^2; resolution =0.6×0.6 mm^2; slice thickness =2 mm; number of slices =40) (16).

Two experienced reviewers (WY, and YS, radiologists with 20 and 3 years of experience, respectively) who were blinded to patients' clinical characteristics independently reviewed all HR-VWI images of carotid arteries. The carotid wall thickness, the volume of plaque components, and the Maximum area percentage of plaque components

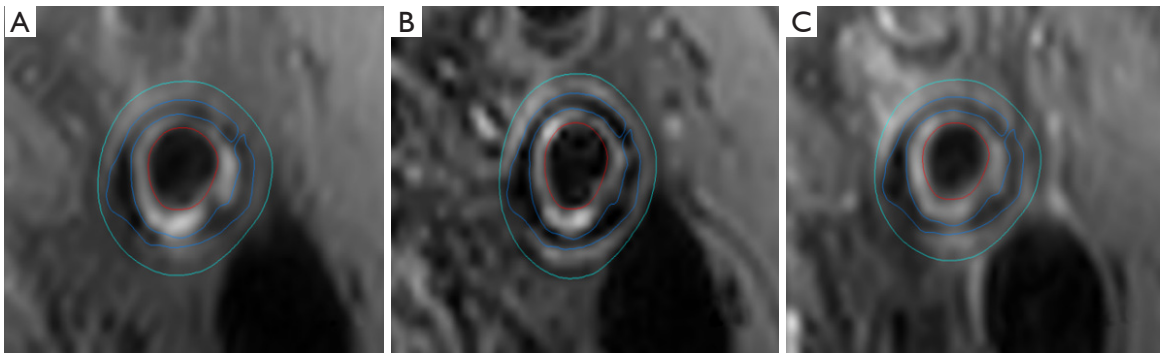

Figure 2 The HR-VWI images of heavy circumferential calcification of the carotid artery. Vessel walls are shown by the green lines. Vessel lumens are shown by the red lines. The presence of calcification is shown by the blue lines. Calcification shows hypointense areas on the HR-VWI images. The calcification circumference involved 4 quadrants. (A) T1-weighted imaging; (B) T2-weighted imaging; (C) post-contrast T1WI. HR-VWI, high-resolution magnetic resonance vessel wall imaging.

were measured on the cross-sectional slices of HR-VWI with commercialized software (Vessel Explorer 2, TSimaging Healthcare, Beijing, China). Lumen and wall boundaries were manually outlined section by section. Wall thickness was automatically measured by the software as the distance between the lumen and wall boundaries. Maximum wall thickness (WT_{max}) and mean wall thickness (WT_{mean}) were automatically by the software measured and calculated. The presence or absence of carotid plaque components, such as calcification, lipid-rich necrotic core (LRNC), and intraplaque hemorrhage (IPH) was evaluated based on the published criteria (16). Calcification shows hypointense areas on all sequences. Due to methemoglobin's comparatively short T1 throughout the subacute and chronic periods, IPH looks bright on T1WI and SNAP. On T2WI, LRNC might be seen as a focal hypointense area. On contrast-enhanced T1WI, LRNC reveals a localized non-enhancing zone within the carotid artery wall. On the cross-sectional slices of HR-VWI, the plaque components were manually outlined section by section. The volume and Maximum area percentage of plaque components were also automatically by the software calculated. To investigate interobserver and intra-observer repeatability, the HR-VWI imaging of 40 chosen random patients was reevaluated by 2 reviewers (Y.S. and Y.X) six months after the initial evaluation.

A previous study used computer tomography (CT) to assess the degree of calcification circumference (17). We used the same criteria to assess the calcification circumference. A 5-point grading system was used to grade the calcification circumference: 0, none; 1, <90° of artery circumference; 2, 90° to 180° of artery circumference; 3, 180° to 270° of artery circumference; and 4, >270° of artery circumference (*Figure 2*). The maximum single-slice calcification circumference score was calculated. Carotid calcification was categorized into four types in accordance with the arrangement of calcification location: surface, interior calcification, bottom, and non-calcification. Surface calcification was defined as calcification located in contact with the lumen, bottom calcification was defined as calcification located within the plaque and away from the lumen, and interior calcification was between the two (17). The calcification location was scored on a 4-point grading scale: 0, none; 1, bottom calcification; 2, interior calcification; 3, superficial calcification. Total calcification location scores were calculated.

CAS implantation and analysis

The procedure was performed according to the previously published protocol (9). Aspirin (100 mg), clopidogrel (75 mg), or ticlopidine (250 mg) were routinely administered for three days before to CAS. Patients who had had anesthesia underwent the procedures. All of the patients received either SpiderFx (ev3, Plymouth, MN, USA) or Filterwire EZ (Boston Scientific, Natick, MA, USA) embolic protection devices (EPDs). The doctors selected stents taking into account the geometry of the lesion, vascular architecture, plaque characteristics, implant features, and operational experience. In the stenotic lesion, open cell stents (Protégé, ev3, Plymouth, Minnesota) or closed cell stents (Wallstent; Boston Scientific, Marlborough, MA) were implanted in all the individuals. A suitable balloon (such as Sterling Boston) was selected

according to the internal carotid artery (ICA) diameter displayed on the digital subtraction angiography (DSA). Based on the physician's judgment, preoperative balloon dilation was used when carotid stenosis interfered with the passage of EPDs and the stent delivery system; postoperative balloon dilation was used when the residual stenosis rate after CAS was >50%. The balloon dilatation pressure is generally used at its nominal pressure level, about 6–8 atm. After the procedure, all patients received aspirin for the rest of their lives along with any type of double or treble antiplatelet medication for at least 3 months.

Two experienced reviewers (LK, and SW, vascular surgeons with 25 and 5 years of experience, respectively) who were blinded to patients' clinical characteristics independently reviewed the DSA images at a workstation (AW4.7; General Electric Healthcare). Carotid artery diameters were manually measured by LK and SW at the workstation before and after CAS (18). The pre-CAS parameters included the residual diameter at the maximal stenosis site and the original carotid artery diameter. The post-CAS parameters included the inner stent diameter at the same stenosis segment. Carotid artery stenosis rates were calculated using DSA with the following equation: the preoperative stenosis rate (%) = (1 – residual diameter/original diameter) ×100%; the post-stenting stenosis rate/residual stenosis rate (%) = (1 – inner stent diameter/original diameter) ×100%. The SER (%) = (preoperative stenosis rate–the residual stenosis rate post stenting) ×100% (6).

Statistical analysis

We used the Shapiro-wilk test to define the normality of the quantitative data distribution. Quantitative data with normal distributions were expressed as means ± standard deviation, and quantitative data that did not conform to normal distribution were expressed as the median [interquartile range (IQR)]. The qualitative data were expressed as percentages. SER had a normal distribution and was analyzed as a continuous variable. The imaging variables with P<0.10 in the simple linear regression analysis were included in the following analysis: multivariable linear regression analysis was used to determine the imaging findings associated with SER of open-cell and closed-cell stents. All analyses were considered significant when the two-sided P value was less than 0.05. The reproducibility of inter-observer and intra-observer results for HR-VWI was evaluated using the intraclass correlation coefficient (ICC). ICC values between 0.6 and 0.75 suggest good reproducibility, above 0.75 imply excellent reproducibility, and values below 0.4 show poor reproducibility. All statistical analyses were performed using commercial SPSS software (IBM SPSS Statistics for Windows, Version 25.0; IBM Corp., Armonk, NY).

Results

Patient baseline and imaging findings

A total of 89 patients (mean age, 70±8 years; 69 men) were included in the final analysis. Among 89 patients, 35 patients were treated with open-cell stents. Fifty-four patients were treated with closed-cell stents. *Table 1* displays the baseline and imaging findings of the study population.

The imaging findings associated with SER of open-cell stents

In simple linear regression analysis, the Maximum single-slice calcification circumference score was associated with a 10.39% lower SER of open-cell stents (95% CI: −19.39 to −1.33; P=0.02). In addition, WT_{max} was associated with a 3.87% lower SER of open-cell stents (95% CI: −7.75 to 0.01; P=0.05), and total calcification location score was associated with a 1.16% lower SER (95% CI: −2.36 to 0.03; P=0.05), although this was borderline in terms of statistical significance. Incorporating maximum single-slice calcification circumference score, WT_{max}, and total calcification location score into multivariable linear regression. The results of the multivariable linear regression revealed that only the maximum single-slice calcification circumference score was the imaging findings associated with SER of open-cell stents (*Table 2*, *Figure 3*). Maximum single-slice calcification circumference score was associated with a 9.35% lower SER of open-cell stents (95% CI: −18.15 to −0.56; P=0.03).

The imaging findings associated with SER of closed-cell stents

Overall, several imaging findings were significantly associated with SER of closed-cell stents in simple linear regression analysis, including WT_{max}, maximum area percentage of calcification, calcification volume, and maximum single-slice calcification circumference score (all P<0.05). WT_{max} was associated with a 3.35% lower SER of closed-cell stents (95% CI: −6.02 to −0.68; P=0.01). The maximum area percentage of calcification was associated

Table 1 Baseline and imaging findings of the study population

Variable	Open-cell stents (n=35)	Closed-cell stents (n=54)
Age, mean ± standard deviation (years)	67.8±7.6	70.8±8.0
Male, n (%)	24 (68.6)	45 (83.3)
Hypertension, n (%)	27 (77.1)	40 (74.1)
Hyperlipidemia, n (%)	25 (71.4)	44 (81.5)
Diabetes, n (%)	9 (25.7)	25 (46.3)
Coronary artery disease, n (%)	6 (17.1)	23 (42.6)
History of stroke, n (%)	8 (22.9)	19 (35.2)
Smoking, n (%)	20 (57.1)	37 (68.5)
Pre-dilatation balloon frequency, n (%)		
1	2 (5.7)	11 (20.4)
2	31 (88.6)	38 (70.4)
3	2 (5.7)	5 (9.3)
Post-dilatation balloon, n (%)	22 (62.9)	35 (64.8)
Preoperative stenosis rate, mean ± standard deviation (%)	69±8.1	68±12.2
WT_{max}, median (IQR) (mm)	5.9 (4.7–7.7)	6.1 (4.8–7.5)
Mean WT, mean ± standard deviation (mm)	2.1±0.4	2.3±0.3
Maximum area percentage of calcification, median (IQR) (%)	10.7 (3.9–18.4)	13.5 (6.2–19.5)
Maximum area percentage of LRNC, median (IQR) (%)	35.4 (0.9–62.2)	36.9 (15.0–54.5)
Maximum area percentage of IPH, median (IQR) (%)	3.7 (0.6–17.3)	14.6 (4.3–31.7)
Calcification volume, median (IQR) (mm^3)	38.2 (13.2–80.1)	53.1 (15.1–102.8)
LRNC volume, median (IQR) (mm^3)	199.7 (0.8–419.8)	173.8 (33.7–461.1)
IPH volume, median (IQR) (mm^3)	6.0 (2.3–81.2)	49.5 (6.2–141.3)
Maximum single-slice calcification circumference score, median (IQR)	2.0 (1.0–3.0)	2.0 (1.0–3.0)
Total calcification location score, median (IQR)	6.0 (3.0–10.0)	7.5 (4.0–11.0)

WT, wall thickness; LRNC, lipid-rich necrotic core; IPH, intraplaque hemorrhage; IQR, interquartile range.

with an 0.83% lower SER of closed-cell stents (95% CI: −1.28 to −0.38; P<0.001). Calcification volume was associated with a 0.02% lower SER of closed-cell stents (95% CI: −0.05 to 0.01; P=0.04). Maximum single-slice calcification circumference score was associated with an 8.67% lower SER of closed-cell stents (95% CI: −12.38 to −4.96; P<0.001). In addition, the total calcification location score was associated with a 0.55% lower SER of closed-cell stents (95% CI: −1.25 to 0.14; P=0.07). Incorporating WT_{max}, maximum area percentage of calcification, calcification volume, maximum single-slice calcification circumference score, and total calcification location score into multivariable linear regression. The results of the multivariable linear regression revealed that the Maximum area percentage of calcification, Maximum single-slice calcification circumference score, and total calcification location score were the imaging findings associated with SER of closed-cell stents (*Table 3*, *Figure 4*). The maximum area percentage of calcification was associated with a 0.67% lower SER of closed-cell stents (95% CI: −1.29 to −0.05; P=0.03). Maximum single-slice calcification circumference score was associated with an 8.43% lower SER of closed-cell stents (95% CI: −13.36 to −3.49; P=0.001). The total calcification location score was associated with a 0.37% lower SER of closed-cell stents (95% CI: −1.08 to 0.09; P=0.02).

Table 2 Simple and multivariable linear regression analysis of SER in open cell stents

Variables	Simple linear regression			Multivariable linear regression		
	β	95% CI	P	β	95% CI	P
WT_{max}	–3.87	–7.75 to 0.01	0.05	–3.37	–7.08 to 0.33	0.07
Mean WT	–15.34	–34.95 to 4.27	0.12			
Maximum area percentage of calcification	–0.70	–1.74 to 0.33	0.17			
Maximum area percentage of LRNC	–0.06	–0.37 to 0.23	0.65			
Maximum area percentage of IPH	–0.11	–0.70 to 0.48	0.70			
Calcification volume	–0.06	–0.18 to 0.05	0.26			
LRNC volume	–0.004	–0.03 to 0.02	0.80			
IPH volume	–0.01	–0.12 to 0.10	0.85			
Maximum single-slice calcification circumference score	–10.39	–19.39 to –1.33	0.02	–9.35	–18.15 to –0.56	0.03
Total calcification location score	–1.16	–2.36 to 0.03	0.05	–0.71	–2.26 to –0.83	0.35

WT, wall thickness; LRNC, lipid-rich necrotic core; IPH, intraplaque hemorrhage; SER, stent expansion rate; CI, confidence interval.

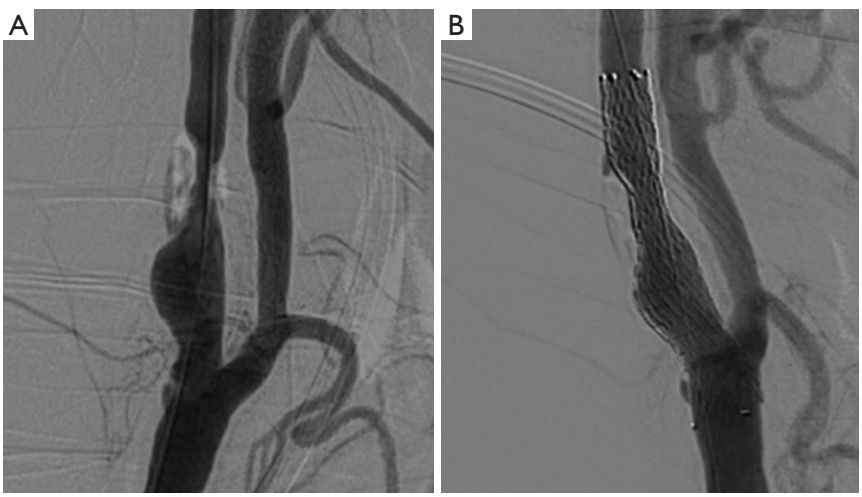

Figure 3 The effect of calcification circumference on SER of open-cell stents. A 76-year-old female patient was treated with open-cell stents (eV3 Protégé RX). (A,B) The corresponding DSA images before and after carotid stenting. The calcification circumference involved 4 quadrants. Heavy circumferential calcification affects the expansion of the open-cell stents. SER, stent expansion rate; DSA, digital subtraction angiography.

Reproducibility evaluation

The inter-observer reproducibility was excellent for WT_{max} (ICC, 0.87; 95% CI, 0.70 to 0.92), WT_{mean} (ICC, 0.84; 95% CI, 0.71 to 0.90), maximum area percentage of calcification (ICC, 0.88; 95% CI, 0.72 to 0.91), maximum area percentage of LRNC (ICC, 0.89; 95% CI, 0.81 to 0.93), maximum area percentage of IPH (ICC, 0.84; 95% CI, 0.71 to 0.94), calcification volume (ICC, 0.81; 95% CI, 0.71 to 0.90), LRNC volume (ICC, 0.87; 95% CI, 0.71 to 0.94), IPH volume (ICC, 0.85; 95% CI, 0.73 to 0.92), maximum single-slice calcification circumference score (ICC, 0.88; 95% CI, 0.70 to 0.93), and total calcification location score (ICC, 0.78; 95% CI, 0.68 to 0.86).

Table 3 Simple and multivariable linear regression analysis of SER in closed cell stents

Variables	Simple linear regression			Multivariable linear regression		
	β	95% CI	P	β	95% CI	P
WT_{max}	−3.35	−6.02 to −0.68	0.01	−2.02	−4.48 to 0.43	0.10
WT_{mean}	−7.11	−60.57 to 2.35	0.29			
Maximum area percentage of calcification	−0.83	−1.28 to −0.38	<0.001	-0.67	−1.29 to −0.05	0.03
Maximum area percentage of LRNC	−0.12	−0.33 to −0.07	0.21			
Maximum area percentage of IPH	−0.11	−0.39 to −0.17	0.43			
Calcification volume	−0.02	−0.05 to 0.01	0.04	−0.003	−0.04 to 0.03	0.88
LRNC volume	−0.01	−0.02 to 0.005	0.18			
IPH volume	−0.01	−0.04 to 0.01	0.35			
Maximum single-slice calcification circumference score	−8.67	−12.38 to −4.96	<0.001	−8.43	−13.36 to −3.49	0.001
Total calcification location score	−0.55	−1.25 to 0.14	0.07	−0.37	−1.08 to 0.09	0.02

WT, wall thickness; LRNC, lipid-rich necrotic core; IPH, intraplaque hemorrhage; SER, stent expansion rate; CI, confidence interval.

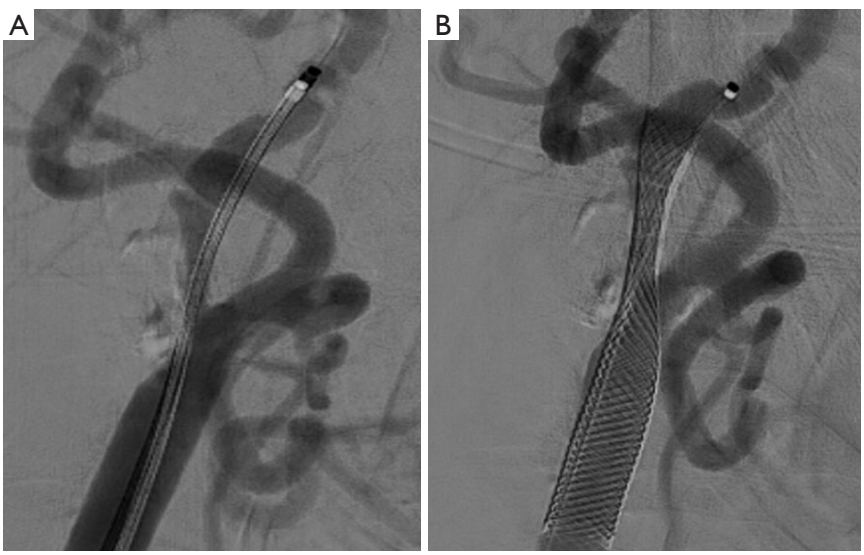

Figure 4 The effect of calcification circumference on SER of closed-cell stents. A 73-year-old male patient was treated with closed-cell stents (Wallstent). (A,B) The corresponding DSA images before and after carotid stenting. The calcification circumference involved 3 quadrants. In the calcified region, the expansion of the closed-cell stents is significantly limited. SER, stent expansion rate; DSA, digital subtraction angiography.

The intra-observer reproducibility was excellent for WT_{max} (ICC, 0.88; 95% CI, 0.71 to 0.92), WT_{mean} (ICC, 0.85; 95% CI, 0.71 to 0.91), maximum area percentage of calcification (ICC, 0.88; 95% CI, 0.73 to 0.90), maximum area percentage of LRNC (ICC, 0.89; 95% CI, 0.82 to 0.94), maximum area percentage of IPH (ICC, 0.85; 95% CI, 0.73 to 0.92), calcification volume (ICC, 0.83; 95% CI, 0.70 to 0.92), LRNC volume (ICC, 0.88; 95% CI, 0.73 to 0.91), IPH volume (ICC, 0.86; 95% CI, 0.74 to 0.93), maximum single-slice calcification circumference score

(ICC, 0.89; 95% CI, 0.73 to 0.93), and total calcification location score (ICC, 0.79; 95% CI, 0.69 to 0.84).

Discussion

According to our research, calcified plaques and SER of the carotid artery are related. Calcification circumference correlates with SER of open-cell stents. Calcification circumference, calcification area, and calcification location are related to the SER of closed-cell stents. We quantified the carotid plaque imaging findings associated with SER by HR-VWI, which may provide a new consideration for clinicians when choosing carotid artery stents.

Calcification has been considered a relative contraindication for CAS and was found to be significantly associated with residual stenosis and restenosis after CAS (6,16,19). Previous studies have shown that the stent expansion is mainly attributable to plaque compression and stretching of the vessel wall (20). Plaque composition can affect stent expansion. The hardness of calcification plaques can resist sufficient plaque compression, which prevents adequate stent expansion (21,22). Our study shows that calcified plaques but not LRNC plaques and IPH plaques are associated with SER of open-cell and closed-cell stents.

Low SER of open-cell and closed-cell stents can occur when the carotid artery wall contains heavy peripheral calcification because the stiff vascular wall generates excessive restriction and stops the placed stent from expanding adequately. Even with comparable calcification volumes, arteries with varied calcification circumferences can sustain various stent expansion strengths due to the eccentricity of the plaque (17,21). This may explain why the calcification volume is not associated with SER of open-cell and closed-cell stents in the multivariate line regression analysis.

Interestingly, we found that the calcification location and the Maximum area percentage of calcification correlated with the SER of the closed-cell stents, but not with the SER of the open-cell stents. We suspect that this is due to open-cell and closed-cell stents having different mechanical properties. An ideal stent will demonstrate good vessel wall adjustment while also dependably covering the plaque. The stent's flexibility and radial force must be sufficient for this purpose (23). However, there are differences in flexibility and radial forces between open-cell and closed-cell stents due to different stent designs and materials (7). Open-cell stents are more flexible and more suited for convoluted arteries is one possible benefit of these devices. Closed-cell stents, on the other hand, have tighter meshes, which could offer greater coverage of the atheromatous lesion but are also stiffer (7). Previous studies found that the flexibility and radial force of closed-cell stents were significantly lower than that of open-cell stents (7,8). In addition, due to their higher stiffness, the closed-cell stents demonstrated poor artery wall adaptation, whereas the open-cell stents adapted significantly better. Worse vessel wall adaptation accompanied by a significant lumen reduction was observed in the closed-cell stents (24). Therefore, we guessed that the high radial force, flexibility, and vessel wall adaptation of the open cell stents may offset the effect of calcification location and calcification area on SER. On the contrary, the SER of closed-cell stents is more susceptible to calcification area due to its low radial force and flexibility. Because the calcifications close to the lumen were frequently irregular, the closed-cell stents and lumen adhesion were weak, resulting in incomplete stent expansion (25). This may explain why the SER of closed-cell stents is more prone to calcification location.

Study limitations

There are some limitations in our study. Firstly, this was a single-center retrospective study and there was a relatively small number of cases. Second, the identification of calcification by HR-VWI also had several limitations. This was because the detection of small surface calcification may be limited by flow artifacts, which TOF is prone to (26). The calcification measured in this study may be underestimated. Third, in this study, we did not further explore the correlation between SER and recurrent stroke, and our future studies will investigate the relationship between the two, which may be more meaningful for the choice of clinical procedure and patient prognosis.

Conclusions

Calcified plaques are associated with SER of the carotid artery. Calcification circumference correlates with SER of open-cell stents. Calcification circumference, calcification area, and calcification location are related to SER of closed-cell stents, which may provide a new consideration for clinicians when choosing carotid artery stents.

Acknowledgments

Funding: This work was supported by the Natural Science

Foundation of Beijing Municipality (No. 7222047 to W Yu) and the China International Medical Exchange Foundation (No. Z-2014-07-2101 to W Yu).

Footnote

Conflicts of Interest: All authors have completed the ICMJE uniform disclosure form (available at https://qims.amegroups.com/article/view/10.21037/qims-22-1215/coif). The authors have no conflicts of interest to declare.

Ethical Statement: The authors are accountable for all aspects of the work in ensuring that questions related to the accuracy or integrity of any part of the work are appropriately investigated and resolved. The study was conducted in accordance with the Declaration of Helsinki (as revised in 2013). The study was approved by the ethics board of Beijing Anzhen Hospital, Beijing, China (No. 2022135X), and individual consent for this retrospective analysis was waived.

References

1. Hoyer UCI, Lennartz S, Abdullayev N, Fichter F, Jünger ST, Goertz L, Laukamp KR, Gertz RJ, Grunz JP, Hohmann C, Maintz D, Persigehl T, Kabbasch C, Borggrefe J, Weiss K, Pennig L. Imaging of the extracranial internal carotid artery in acute ischemic stroke: assessment of stenosis, plaques, and image quality using relaxation-enhanced angiography without contrast and triggering (REACT). Quant Imaging Med Surg 2022;12:3640-54.
2. Brott TG, Hobson RW 2nd, Howard G, Roubin GS, Clark WM, Brooks W, et al. Stenting versus endarterectomy for treatment of carotid-artery stenosis. N Engl J Med 2010;363:11-23.
3. Roh J, Baik SK, Yeom JA, Park KP, Ahn SH, Park MG. Usefulness of cone-beam computed tomography to predict residual stenosis after carotid artery stenting. Interv Neuroradiol 2022. [Epub ahead of print]. doi: 10.1177/15910199221143259.
4. Cheng X, Dong Z, Liu J, Li H, Zhou C, Zhang F, Wang C, Zhang Z, Lu G. Prediction of Carotid In-Stent Restenosis by Computed Tomography Angiography Carotid Plaque-Based Radiomics. J Clin Med 2022;11:3234.
5. AbuRahma AF, AbuRahma ZT, Scott G, Adams E, Mata A, Beasley M, Dean LS, Davis E. The incidence of carotid in-stent stenosis is underestimated ≥50% or ≥80% and its clinical implications. J Vasc Surg 2019;69:1807-14.
6. Tao Y, Hua Y, Jia L, Jiao L, Liu B. Risk Factors for Residual Stenosis After Carotid Artery Stenting. Front Neurol 2021;11:606924.
7. Wissgott C, Schmidt W, Behrens P, Brandt C, Schmitz KP, Andresen R. Experimental investigation of modern and established carotid stents. Rofo 2014;186:157-65.
8. Voûte MT, Hendriks JM, van Laanen JH, Pattynama PM, Muhs BE, Poldermans D, Verhagen HJ. Radial force measurements in carotid stents: influence of stent design and length of the lesion. J Vasc Interv Radiol 2011;22:661-6.
9. Mazurek A, Malinowski K, Rosenfield K, Capoccia L, Speziale F, de Donato G, et al. Clinical Outcomes of Second- versus First-Generation Carotid Stents: A Systematic Review and Meta-Analysis. J Clin Med 2022;11:4819.
10. Geiger MA, Flumignan RLG, Sobreira ML, Avelar WM, Fingerhut C, Stein S, Guillaumon AT. Carotid Plaque Composition and the Importance of Non-Invasive in Imaging Stroke Prevention. Front Cardiovasc Med 2022;9:885483.
11. Tapis P, El-Koussy M, Hewer E, Mono ML, Reinert M. Plaque vulnerability in patients with high- and moderate-grade carotid stenosis - comparison of plaque features on MRI with histopathological findings. Swiss Med Wkly 2020;150:w20174.
12. Zhang D, Wang M, Wu L, Zhao Y, Wang S, Yin X, Wu X. Assessing the characteristics and diagnostic value of plaques for patients with acute stroke using high-resolution magnetic resonance imaging. Quant Imaging Med Surg 2022;12:1529-38.
13. Fabiano S, Mancino S, Stefanini M, Chiocchi M, Mauriello A, Spagnoli LG, Simonetti G. High-resolution multicontrast-weighted MR imaging from human carotid endarterectomy specimens to assess carotid plaque components. Eur Radiol 2008;18:2912-21.
14. Barnett HJ, Taylor DW, Eliasziw M, Fox AJ, Ferguson

GG, Haynes RB, Rankin RN, Clagett GP, Hachinski VC, Sackett DL, Thorpe KE, Meldrum HE, Spence JD. Benefit of carotid endarterectomy in patients with symptomatic moderate or severe stenosis. North American Symptomatic Carotid Endarterectomy Trial Collaborators. N Engl J Med 1998;339:1415-25.
15. Li D, Dai W, Cai Y, Han Y, Yao G, Chen H, Yuan C, Xiao L, Zhao X. Atherosclerosis in stroke-related vascular beds and stroke risk: A 3-D MR vessel wall imaging study. Ann Clin Transl Neurol 2018;5:1599-610.
16. Saba L, Yuan C, Hatsukami TS, Balu N, Qiao Y, DeMarco JK, Saam T, Moody AR, Li D, Matouk CC, Johnson MH, Jäger HR, Mossa-Basha M, Kooi ME, Fan Z, Saloner D, Wintermark M, Mikulis DJ, Wasserman BA; Vessel Wall Imaging Study Group of the American Society of Neuroradiology. Carotid Artery Wall Imaging: Perspective and Guidelines from the ASNR Vessel Wall Imaging Study Group and Expert Consensus Recommendations of the American Society of Neuroradiology. AJNR Am J Neuroradiol 2018;39:E9-31.
17. Lv P, Ji A, Zhang R, Guo D, Tang X, Lin J. Circumferential degree of carotid calcification is associated with new ischemic brain lesions after carotid artery stenting. Quant Imaging Med Surg 2021;11:2669-76.
18. Tan Q, Qin C, Yang J, Wang T, Lin H, Lin C, Chen X. Inner diameters of the normal carotid arteries measured using three-dimensional digital subtraction catheter angiography: a retrospective analysis. BMC Neurol 2021;21:292.
19. Kim CH, Kang J, Ryu WS, Sohn CH, Yoon BW. Effects of Carotid Calcification on Restenosis After Carotid Artery Stenting: A Follow-Up Study with Computed Tomography Angiography. World Neurosurg 2018;117:e514-21.
20. Elsayed N, Yei KS, Naazie I, Goodney P, Clouse WD, Malas M. The impact of carotid lesion calcification on outcomes of carotid artery stenting. J Vasc Surg 2022;75:921-9.
21. Barrett HE, Cunnane EM, Kavanagh EG, Walsh MT. On the effect of calcification volume and configuration on the mechanical behaviour of carotid plaque tissue. J Mech Behav Biomed Mater 2016;56:45-56.
22. Fukushima D, Kondo K, Harada N, Terazono S, Uchino K, Shibuya K, Sugo N. Quantitative comparison between carotid plaque hardness and histopathological findings: an observational study. Diagn Pathol 2022;17:58.
23. de Vries EE, Kök M, Hoving AM, Slump CH, Toorop RJ, de Borst GJ. (In)comparability of Carotid Artery Stent Characteristics: A Systematic Review on Assessment and Comparison with Manufacturer Data. Cardiovasc Intervent Radiol 2020;43:1430-7.
24. Wissgott C, Schmidt W, Brandt-Wunderlich C, Behrens P, Andresen R. Clinical Results and Mechanical Properties of the Carotid CGUARD Double-Layered Embolic Prevention Stent. J Endovasc Ther 2017;24:130-7.
25. Katano H, Mase M, Nishikawa Y, Yamada K. Surgical treatment for carotid stenoses with highly calcified plaques. J Stroke Cerebrovasc Dis 2014;23:148-54.
26. Lin R, Chen S, Liu G, Xue Y, Zhao X. Association Between Carotid Atherosclerotic Plaque Calcification and Intraplaque Hemorrhage: A Magnetic Resonance Imaging Study. Arterioscler Thromb Vasc Biol 2017;37:1228-33.

Cite this article as: Sun Y, Xu H, Kou L, Wang S, Wang Z, Yu W. Calcification circumference, area, and location are associated with carotid stent expansion rate: high-resolution magnetic resonance vessel wall imaging study. Quant Imaging Med Surg 2023;13(7):4493-4503. doi: 10.21037/qims-22-1215

